Infectious disease prediction with kernel conditional density estimation Supplementary Material

Evan L. Ray[1], Krzysztof Sakrejda[1], Stephen A. Lauer[1],
Michael A. Johansson[2], Nicholas G. Reich[1]

[1] *Department of Biostatistics and Epidemiology,*
School of Public Health and Health Sciences,
University of Massachusetts, Amherst
415 Arnold House, 715 N. Pleasant Street, Amherst, MA 01003, USA

[2] *Dengue Branch, Division of Vector-Borne Infectious Diseases,*
Centers for Disease Control and Prevention,
San Juan, Puerto Rico, USA

1 Methodological Details

1.1 Discretizing the Kernel Function

We obtain the discrete kernel function by discretizing an underlying continuous kernel function. For each component of the vector $\tilde{\mathbf{z}}_{t^*} = (z_{t^*-l_1}, \ldots, z_{t^*-l_M}, z_{t^*+h})'$, we associate lower and upper bounds of integration a_{z_j} and b_{z_j} with each value in the domain of that random variable. The value of the kernel function is obtained by integrating over the hyper-rectangle specified by these bounds:

$$K_{\text{disc}}^{\text{inc}}(\tilde{\mathbf{z}}_{t^*}, \tilde{\mathbf{z}}_t; \mathbf{B}^h) = \int_{a_{z_{t^*-l_1}}}^{b_{z_{t^*-l_1}}} \cdots \int_{a_{z_{t^*+h}}}^{b_{z_{t^*+h}}} K_{\text{cont}}^{\text{inc}}(\tilde{\mathbf{z}}_{t^*}, \tilde{\mathbf{z}}_t; \mathbf{B}^h) \, dz_{t^*-l_1} \cdots dz_{t^*+h}.$$

In our application, the possible values of the random variables are non-negative integer case counts. In order to facilitate use of the log-normal kernel, we add 0.5 to the observed case counts; the corresponding integration bounds are the non-negative integers as illustrated in Figure 2.

1.2 Parameter Estimation

We follow a two-stage strategy for parameter estimation (Joe, 2005):

1. Estimate the parameters for marginal predictive distributions using the cross-validation procedure described in Section 2.1 of the main text.

2. Estimate the copula parameters, holding the parameters for the marginal predictive distributions fixed:

   (a) Form vectors of "pseudo-observations" by passing observed incidence trajectories from previous seasons through the marginal predictive c.d.f.s obtained in step 1:

   $$(u_{k,1}, \ldots, u_{k,H}) =$$
   $$\{F^1(z_{t_k^*+1}|t_k^*, z_{t_k^*-l_1}, \ldots, z_{t_k^*-l_M}; \boldsymbol{\theta}^1), \ldots, F^H(z_{t_k^*+H}|t_k^*, z_{t_k^*-l_1}, \ldots, z_{t_k^*-l_M}; \boldsymbol{\theta}^H)\}$$

We form one such vector of pseudo-observations for each season in the training data; in the notation here, these seasons are indexed by k. The relevant time points t_k^* are the times in those previous seasons falling H time steps before the end of the season.

(b) Estimate the copula parameters $\boldsymbol{\xi}^H$ by maximizing the likelihood of the pseudo-observations.

2 Simulation Study Details

2.1 Simulation Distributions

In the simulation study, we simulate data from discretized multivariate normal distributions. The method for discretizing the underlying multivariate normal is the same as we described above for descritizing the kernel function. As we discussed in the paper, the normal distribution has mean $\underline{0}$ and covariance matrix with 1 on the diagonal and 0.9 off of the diagonal. This multivariate normal distribution was used in one of the simulation studies conducted by Duong and Hazelton [2005] demonstrating that a fully parameterized bandwidth matrix could yield improved density estimates for joint density estimation with continuous distributions. We discretize this distribution at the half-integers as illustrated for the two-dimensional case in Figure 3.

2.2 Hellinger Distance

The Hellinger distance of the estimated density $\widehat{f}(x)$ from the true density $f(x)$ is given by

$$\text{Hellinger}(f, \widehat{f}) = \left[1 - \int \left\{ f(x)\widehat{f}(x) \right\}^{\frac{1}{2}} dx \right]^{\frac{1}{2}}$$

In the simulation study, we measure the quality of a conditional density estimate by integrating the Hellinger distance over the range of the conditioning variables, weighting according to the density of those conditioning variables:

$$
\begin{aligned}
&\text{Score}\{\widehat{f}(x_1|x_2,\ldots,x_D)\} \\
&= \int \cdots \int \left[\text{Hellinger}\{ f(x_1|x_2,\ldots,x_D), \widehat{f}(x_1|x_2,\ldots,x_D) \} \right] f(x_2,\ldots,x_D) dx_2 \cdots dx_D \\
&= \int \cdots \int \left[1 - \int \left\{ f(x_1|x_2,\ldots,x_D)\widehat{f}(x_1|x_2,\ldots,x_D) \right\}^{\frac{1}{2}} dx_1 \right]^{\frac{1}{2}} f(x_2,\ldots,x_D) dx_2 \cdots dx_D \\
&= \int \cdots \int \left[1 - \int \left\{ \frac{\widehat{f}(x_1|x_2,\ldots,x_D)}{f(x_1|x_2,\ldots,x_D)} \right\}^{\frac{1}{2}} f(x_1|x_2,\ldots,x_D) \, dx_1 \right]^{\frac{1}{2}} f(x_2,\ldots,x_D) dx_2 \cdots dx_D
\end{aligned}
$$

$$(1)$$

We perform Monte Carlo integration to evaluate the integrals in Equation (1) by sampling observations $(x_{i,1},\ldots,x_{i,D})$ from the joint distribution of $\mathbf{X}$.

3 Application Details

3.1 Prediction Targets

As we discussed in the main article, there are three prediction targets for each data set:

1. For each week in the test data, we obtain a predictive distribution for the incidence measure in that week at each prediction horizon from 1 to 52 weeks ahead.

2. In each week of the test data set, we make predictions for the timing of the peak week of the corresponding season.

3. In each week of the test data set we predict incidence in the peak week for the corresponding season. Following the precedent set in the competitions, we make predictions for *binned* incidence in the peak week.

These prediction targets are illustrated in Figure 4.

3.2   Predictive Distributions for Individual Weeks: Additional Results

Here we present some additional results for predicting incidence in individual weeks in the applications. Figure 5 shows that including the periodic kernel in the KCDE specification yielded consistent performance gains in the application to influenza. The performance gains in the application to dengue fever were smaller, but average performance was still higher when the periodic kernel was included. The figure also shows that the gains from using a fully parameterized bandwidth instead of a diagonal bandwidth are negligible, though there is a small gain on average in the application to influenza.

3.3   Predictive Distributions for Peak Week and Peak Incidence: Additional Results

Figure 6 in the main text shows log scores for prediction of incidence in the peak week. Figure 6 in this supplement shows the corresponding results for prediction of peak week timing. As with predictions of peak incidence, there is no clear evidence that KCDE either outperforms or underperforms relative to the SARIMA model. The log scores give us information about the values that the predictive distributions take at a single value: the eventual realized outcome. Figures 7 through 10 give more information, about the predictive distributions for peak week height and timing obtained from SARIMA and the Periodic, Full Bandwidth KCDE specification.

As we discussed in the main text, the predictive distributions for peak week timing and incidence are obtained by performing an appropriate Monte Carlo integral of the joint distribution for incidence in all remaining weeks in the season. In more plain language, we sample incidence trajectories from the joint predictive distribution of incidence in all remaining weeks and calculate the proportion of those sampled trajectories where the peak fell in each incidence bin or at each week of the season.

Figure 11 illustrates this with the Periodic, Full Bandwidth KCDE specification and the SARIMA model. For reference, we have also included all observed trajectories for the seasons in the training and test data sets and trajectories sampled from the predictive distribution that would be obtained by combining the KCDE predictions at different horizons using an independence assumption instead of a copula. We can see that the effect of the copula is to induce correlation in the incidence across different weeks. The trajectories obtained with the copula are much smoother than the trajectories obtained with an independence assumption.

3.4   The Christmas Effect

Figure 12 illustrates the consistent peak in reported influenze incidence around Christmas that we have termed the "Christmas effect". This peak is sometimes a short-term spike in reported incidence, and sometimes coincides with the season peak. There are a variety of possible explanations for this effect, such as heightened flu transmission due to increased travel or more reporting of flu relative to other diseases in that time.

Regardless, this is a regular seasonal phenomenon that the structure of the SARIMA model picks up on. We can see this from the horizontal banding in Figure 7. Note that because the disease season is defined to begin in July, Christmas occurs in week 22 of the season. In the predictive distributions for peak week timing from SARIMA, there is a consistent sharp peak at week 22, followed by a

trough in the weeks immediately thereafter and another broader mode in the approximate range of weeks 26 to 33. In other words, the predictive distributions obtained from SARIMA capture the fact that there is likely to be a peak centered at Christmas week, which will be followed by a dip but may be followed by another increase later in the season. The SARIMA model is able to capture this pattern through its use of seasonal differencing and seasonal lags. Our KCDE specification places high probability for peak weeks in the generally correct area, but has not captured this Christmas effect.

We note that the SARIMA model also yields horizontal banding in the predictions for peak week timing for the dengue data, as can be seen from Figure 8. However, there the banding is less informative, and the smoother predictive distributions obtained from KCDE may be preferred from the perspective of communicating with decision makers.

References

Tarn Duong and Martin L Hazelton. Cross-validation bandwidth matrices for multivariate kernel density estimation. *Scandinavian Journal of Statistics*, 32(3):485–506, 2005.

Rob J Hyndman. *forecast: Forecasting functions for time series and linear models*, 2015. URL http://github.com/robjhyndman/forecast. R package version 6.2.

Harry Joe. Asymptotic efficiency of the two-stage estimation method for copula-based models. *Journal of Multivariate Analysis*, 94(2):401–419, 2005.
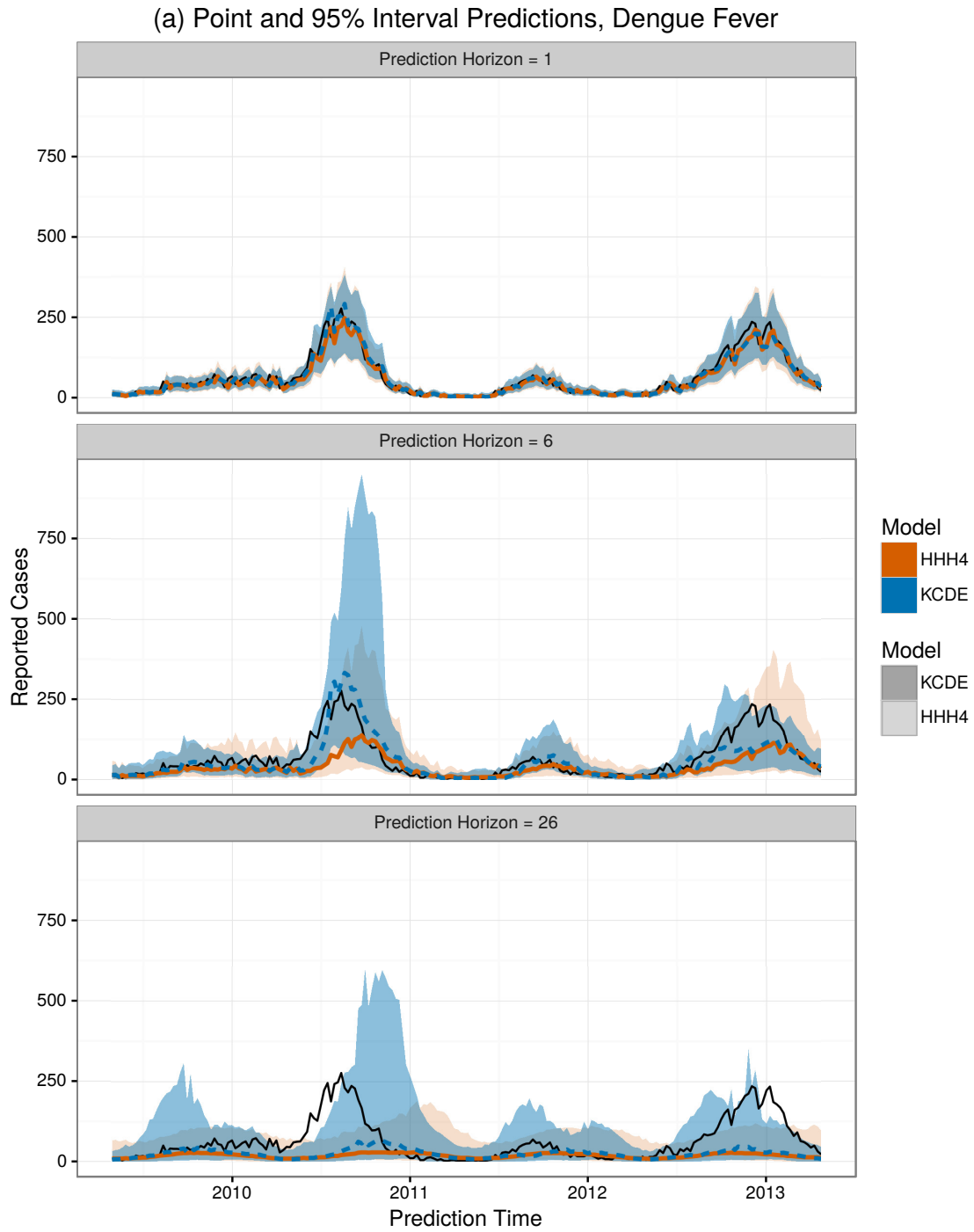
Figure 1: Plots of point and interval predictions from HHH4 and the Periodic, Full Bandwidth KCDE model.
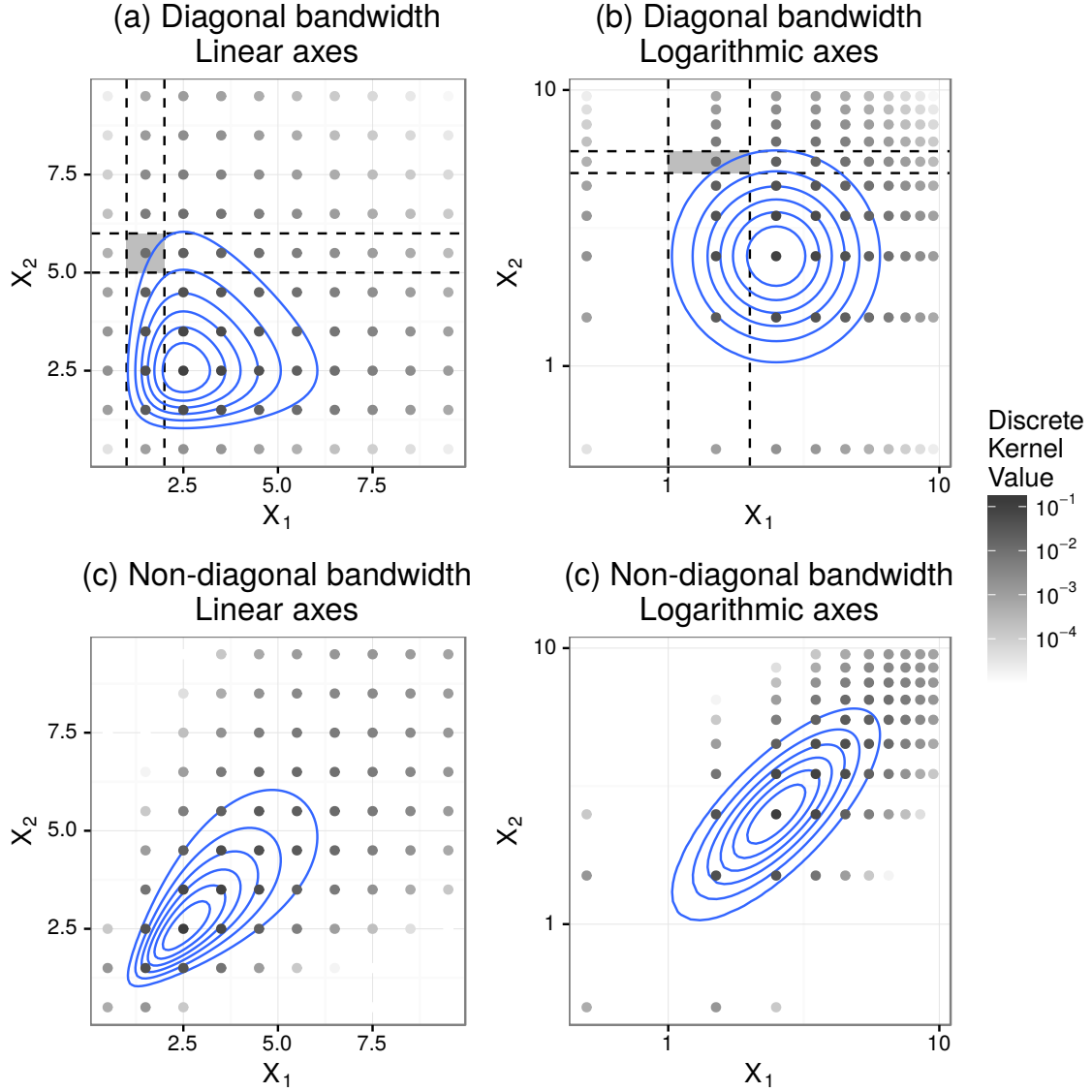
Figure 2: Illustrations of $K_{\text{cont}}^{\text{inc}}$ and $K_{\text{disc}}^{\text{inc}}$ in the bivariate case. Solid lines show contours of the continuous kernel function. Grey dots indicate the value of the discrete kernel function. The value of the discrete kernel is obtained by integrating the continuous kernel over regions as illustrated by the dashed lines in panels (a) and (b). In all panels the kernel function is centered at $(2.5, 2.5)$. Panels (a) and (b) show the same kernel function with different axis scales; the bandwidth matrix is $\begin{bmatrix} 0.2 & 0 \\ 0 & 0.2 \end{bmatrix}$. Panels (c) and (d) show the same kernel function, with bandwidth matrix $\begin{bmatrix} 0.2 & 0.15 \\ 0.15 & 0.2 \end{bmatrix}$.
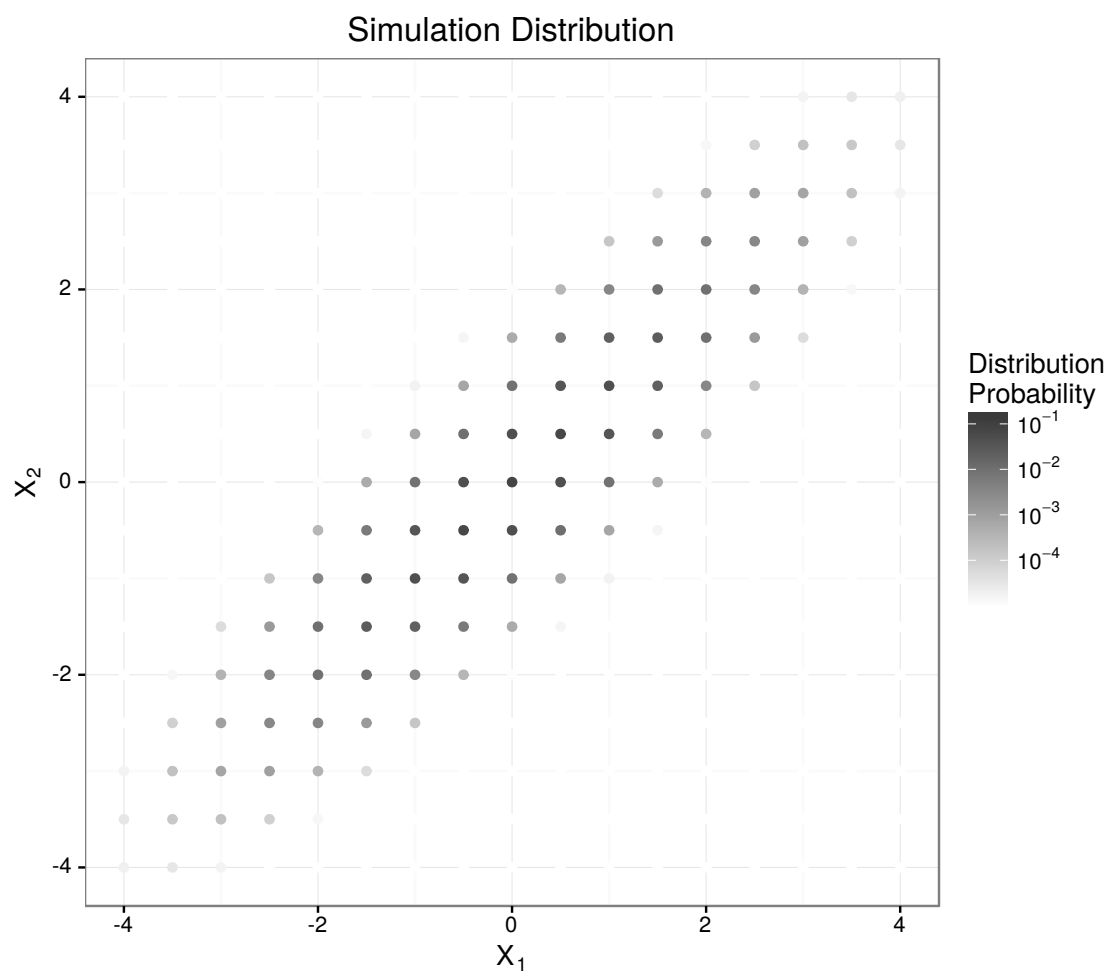
Figure 3: The distribution that we simulate data from in the simulation study.
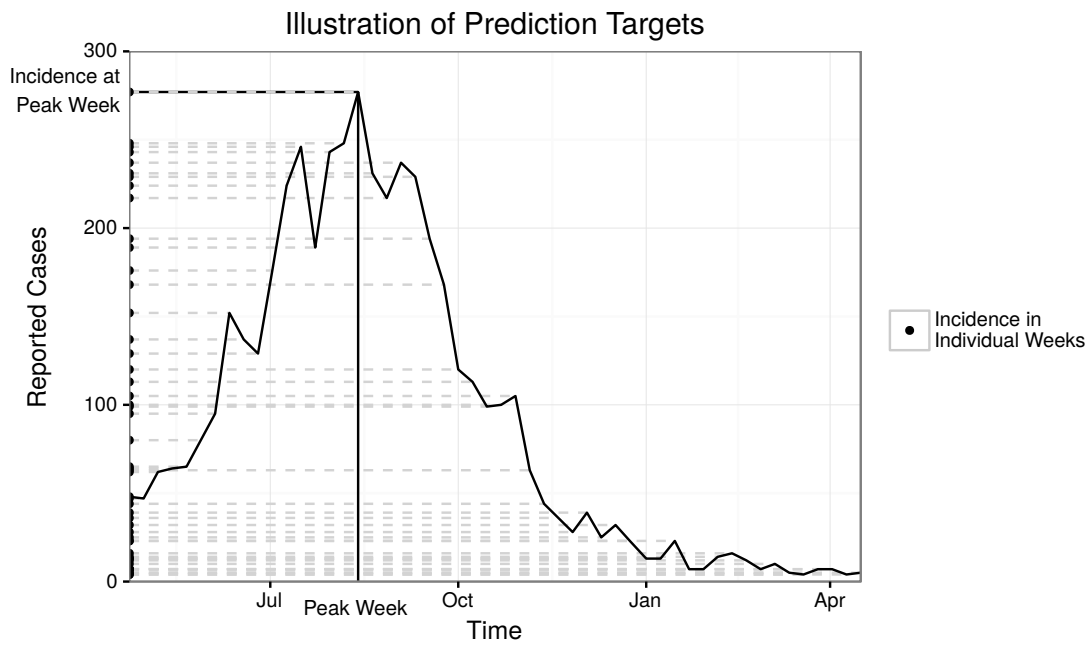
Figure 4: Illustration of the prediction targets using one season of the dengue data. The solid vertical line indicates the timing of the peak week. The solid horizontal line indicates the incidence at the peak week. The points along the vertical axis indicate the incidence at every week for the 52 weeks after the time at which predictions are made.
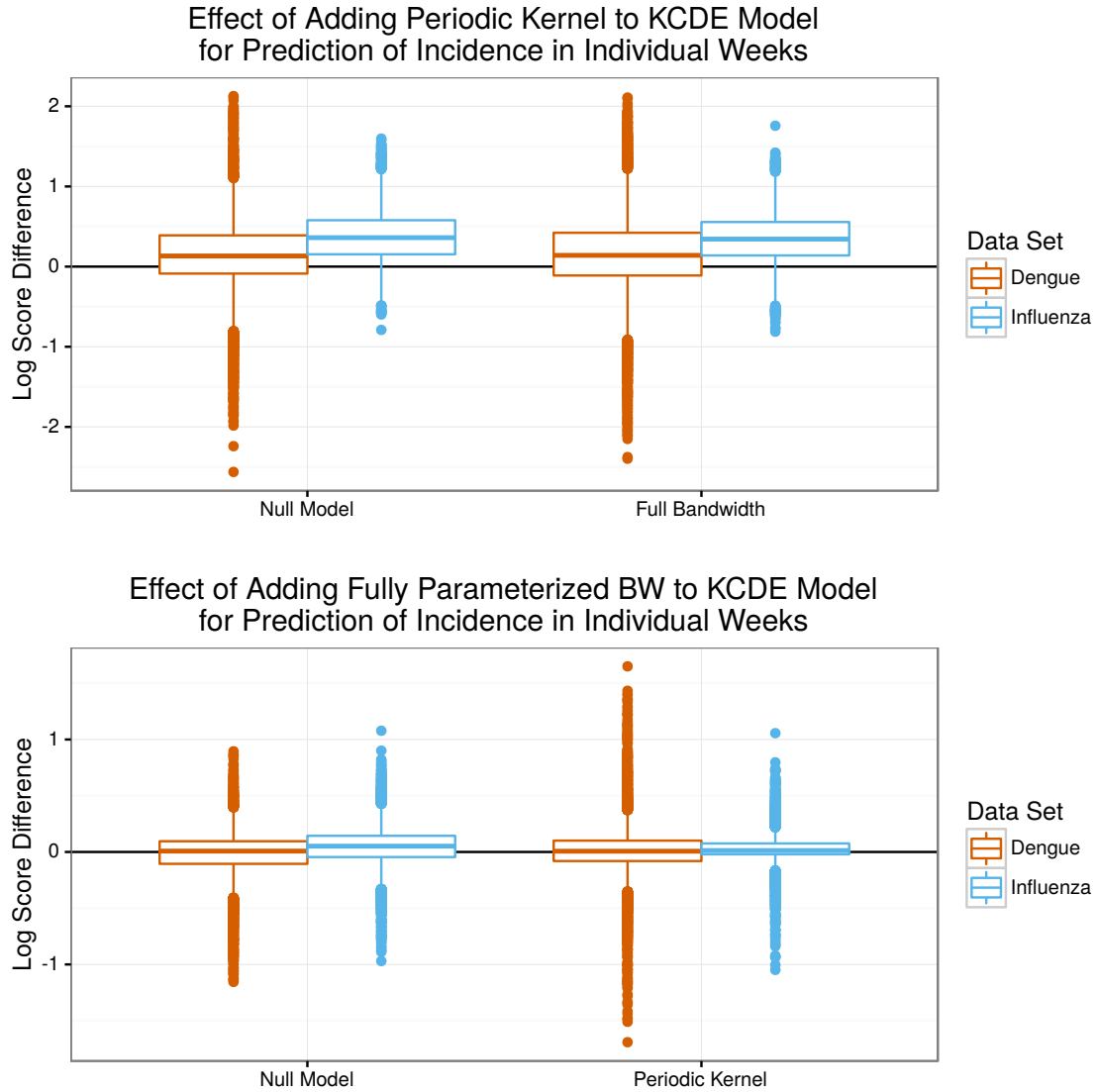
Figure 5: Differences in log scores for the weekly predictive distributions among pairs of models across all combinations of prediction horizon and prediction time in the test period. In the upper panel positive values indicate cases when the specification of KCDE with the periodic kernel outperformed the corresponding specification without the periodic kernel. In the lower panel positive values indicate cases when the specification of KCDE with a fully parameterized bandwidth outperformed the corresponding KCDE specification with a diagonal bandwidth matrix.
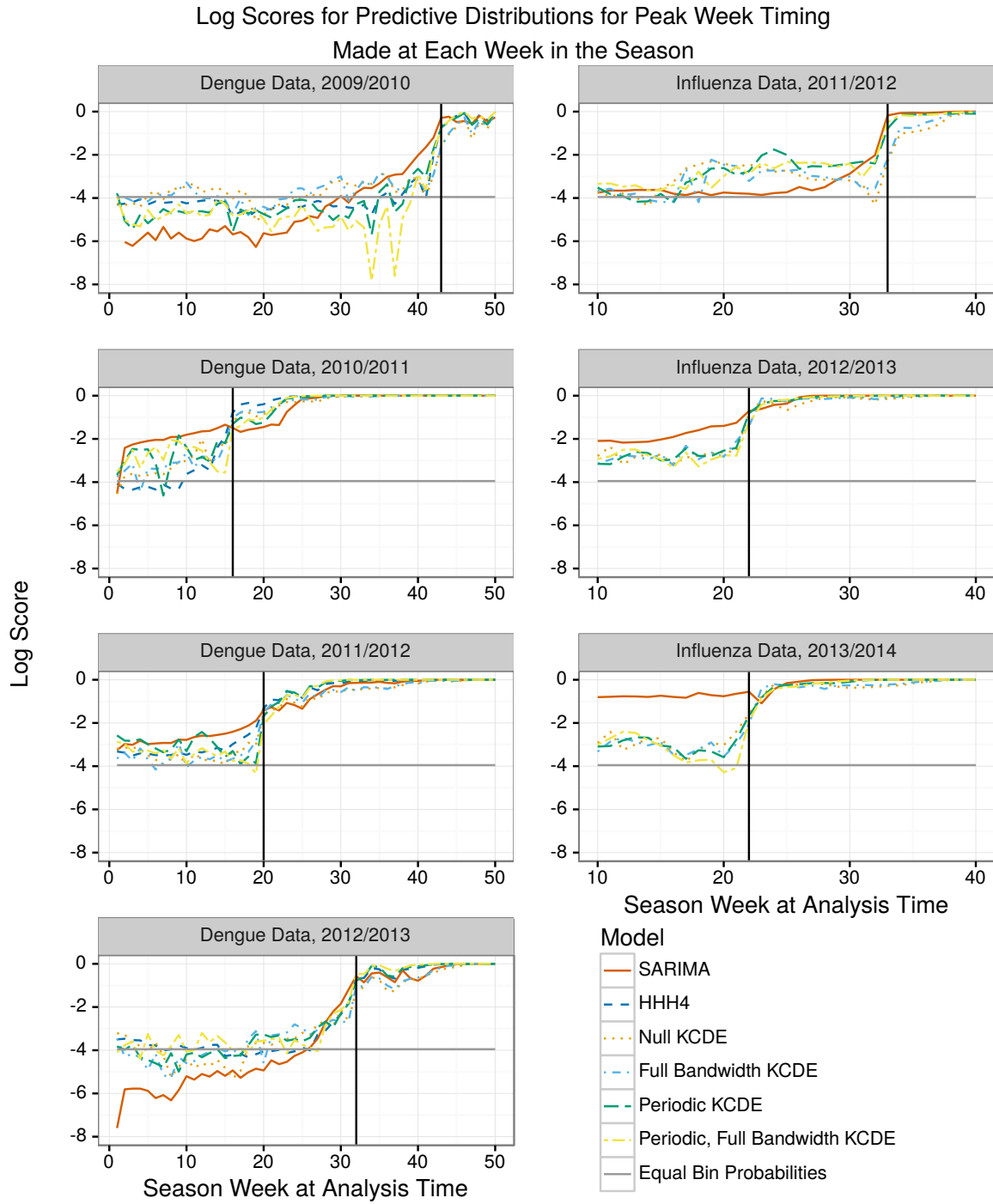
Figure 6: Log scores for predictions of peak week timing by predictive model and analysis time. The vertical line is placed at the peak week for each season. The log score for "Equal Bin Probabilities" is obtained by assigning equal probability that the peak will occur in each week of the year.
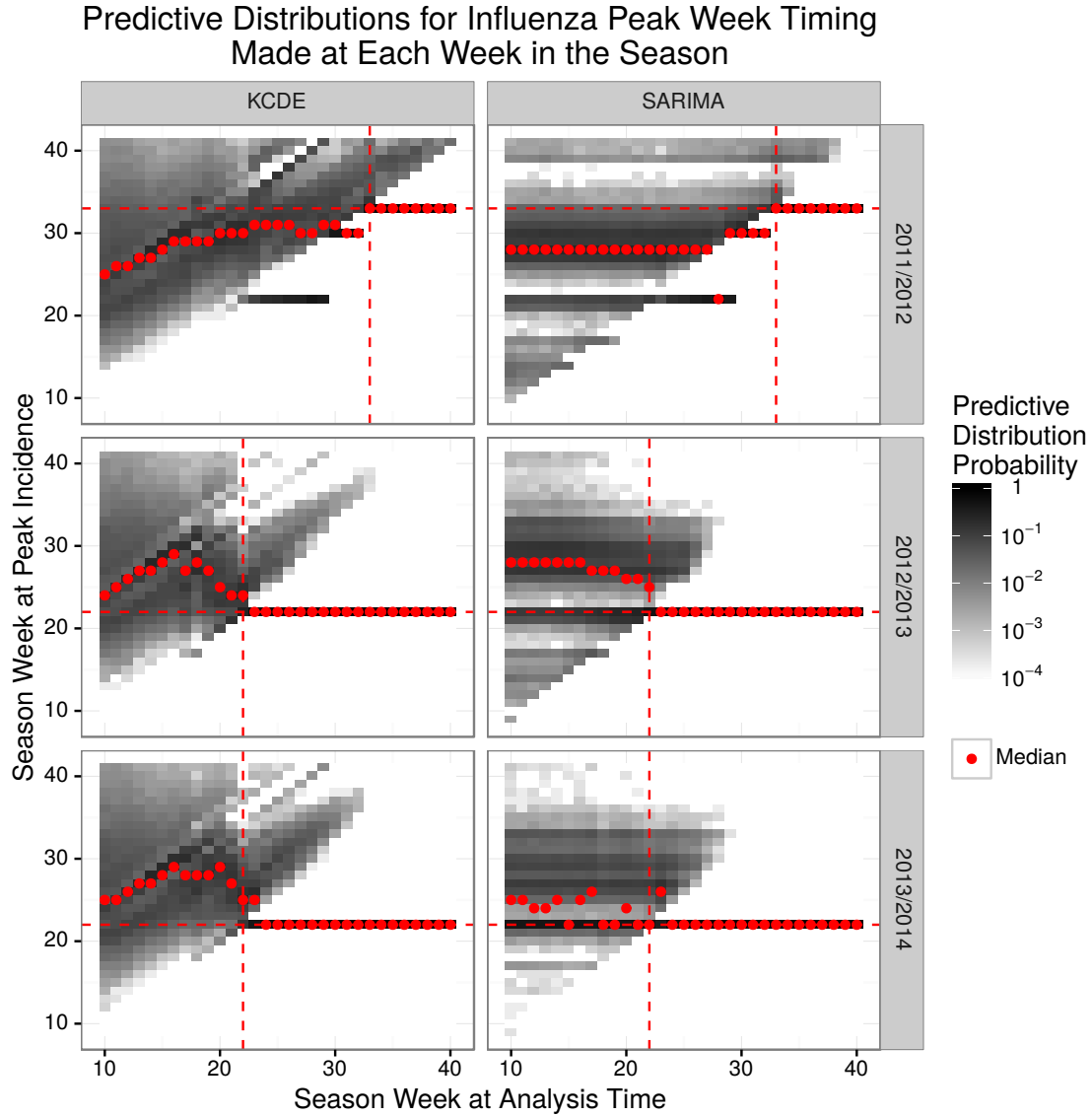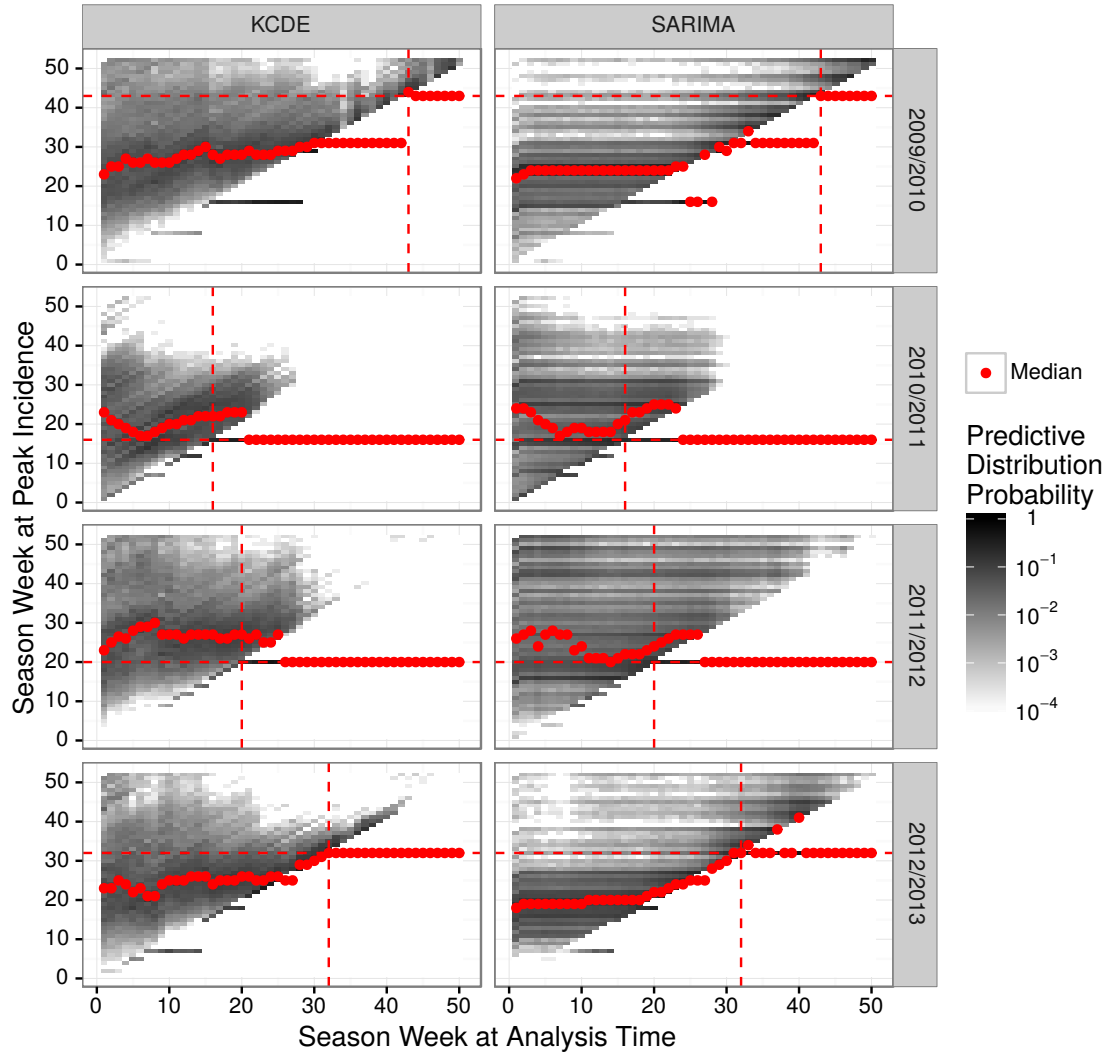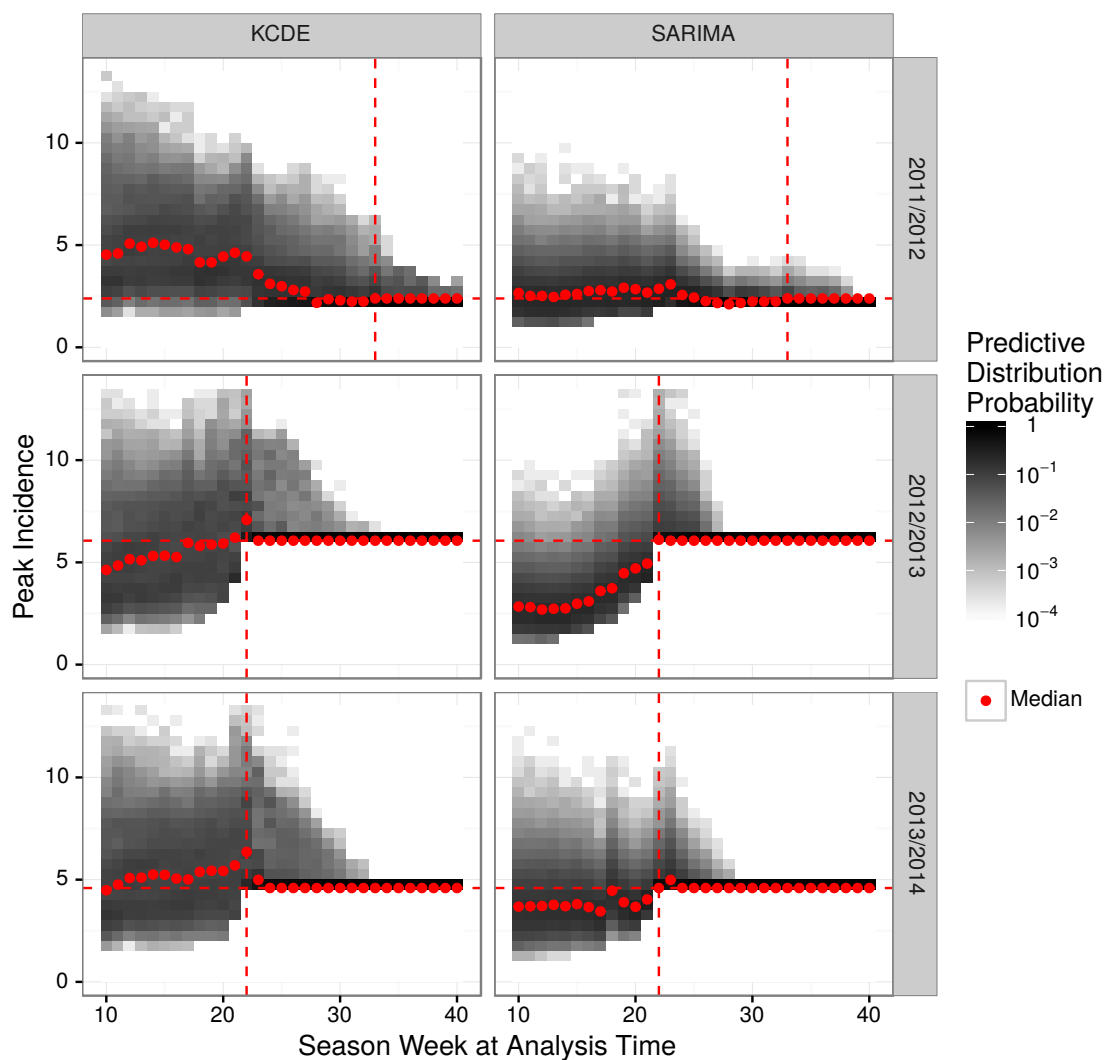
Figure 7: Predictive distributions for predictions of peak week timing for influenza. The horizontal axis represents the week in the season at which the prediction is made. The vertical axis represents weeks in the season at which the peak could potentially occur. Each "column" represents one predictive distribution. The horizontal and vertical dashed lines are at the observed peak week for the season.

Figure 8: Predictive distributions for predictions of peak week timing for dengue fever. The horizontal axis represents the week in the season at which the prediction is made. The vertical axis represents weeks in the season at which the peak could potentially occur. Each "column" represents one predictive distribution. The horizontal and vertical dashed lines are at the observed peak week for the season.

Figure 9: Predictive distributions for predictions of peak week incidence for influenza. The horizontal axis represents the week in the season at which the prediction is made. The vertical axis represents binned incidence in the peak week, as described in the main text. Each "column" represents one predictive distribution. The horizontal dashed line is at the observed peak incidence for the season. The vertical dashed line is at the observed peak week for the season.
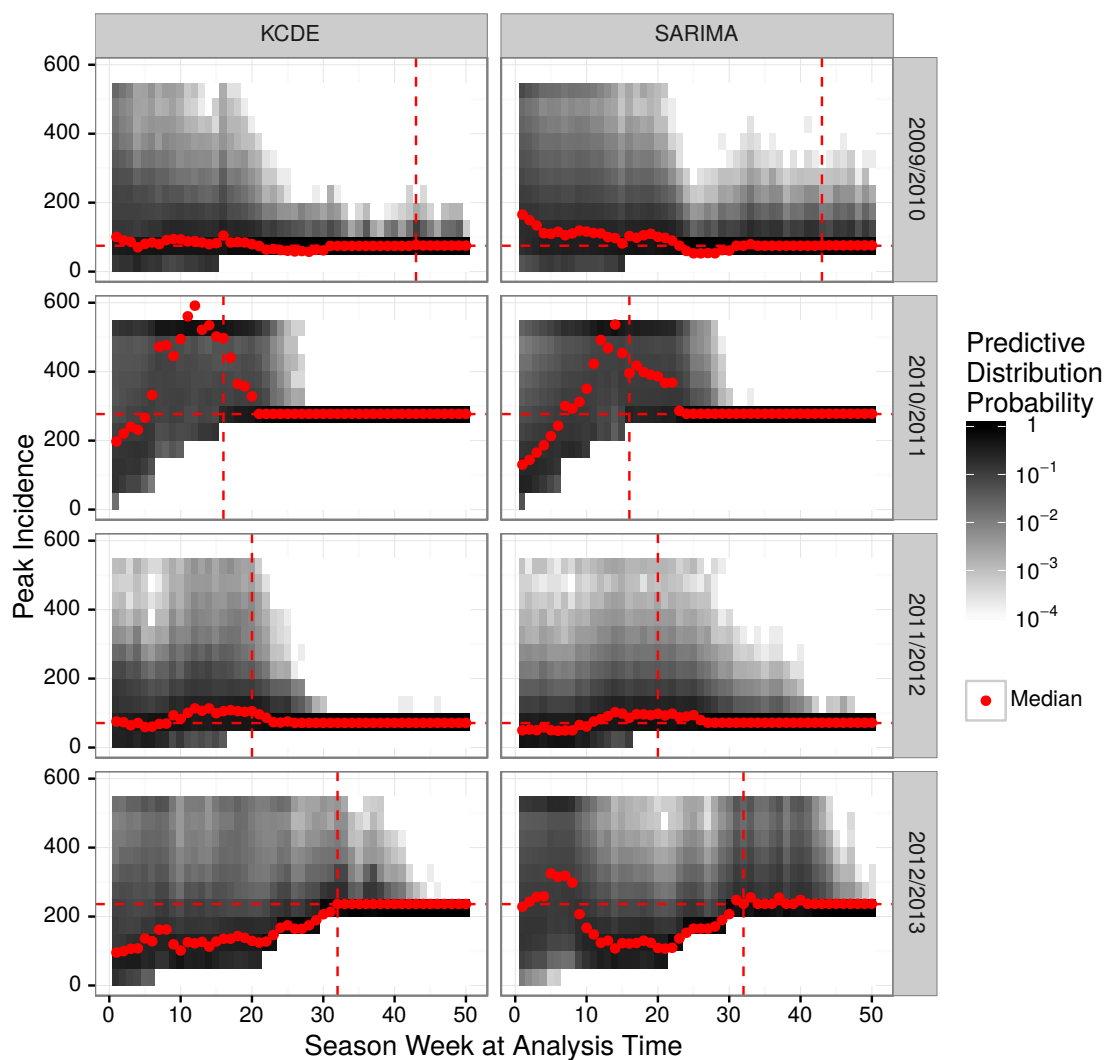
Figure 10: Predictive distributions for predictions of peak week incidence for dengue fever. The horizontal axis represents the week in the season at which the prediction is made. The vertical axis represents binned incidence in the peak week, as described in the main text. Each "column" represents one predictive distribution. The horizontal dashed line is at the observed peak incidence for the season. The vertical dashed line is at the observed peak week for the season.
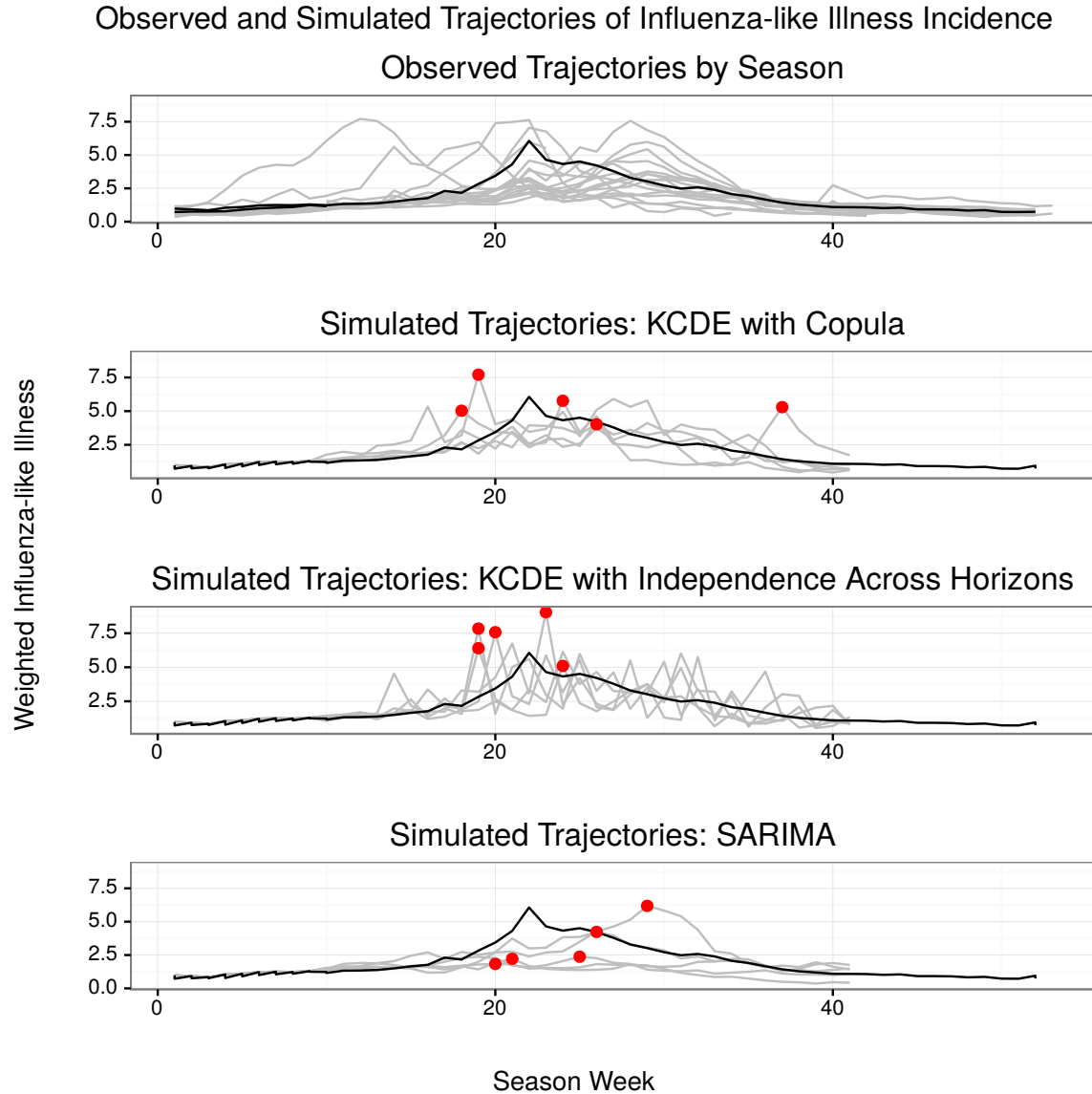
Figure 11: Incidence trajectories for the influenza data set. The top panel displays the observed trajectories for all seasons in the data set, with the 2012/2013 season in darker color. The lower three panels display the observed trajectory from the 2012/2013 season and five simulated incidence trajectories from each of three models: the KCDE model with copula as implemented in our applications; a KCDE model using an independence assumption across prediction horizons; and the SARIMA model. The simulated trajectories are generated from the predictive distribution obtained 10 weeks into the 2012/2013 season. The red points indicate the peak week in each simulated trajectory.
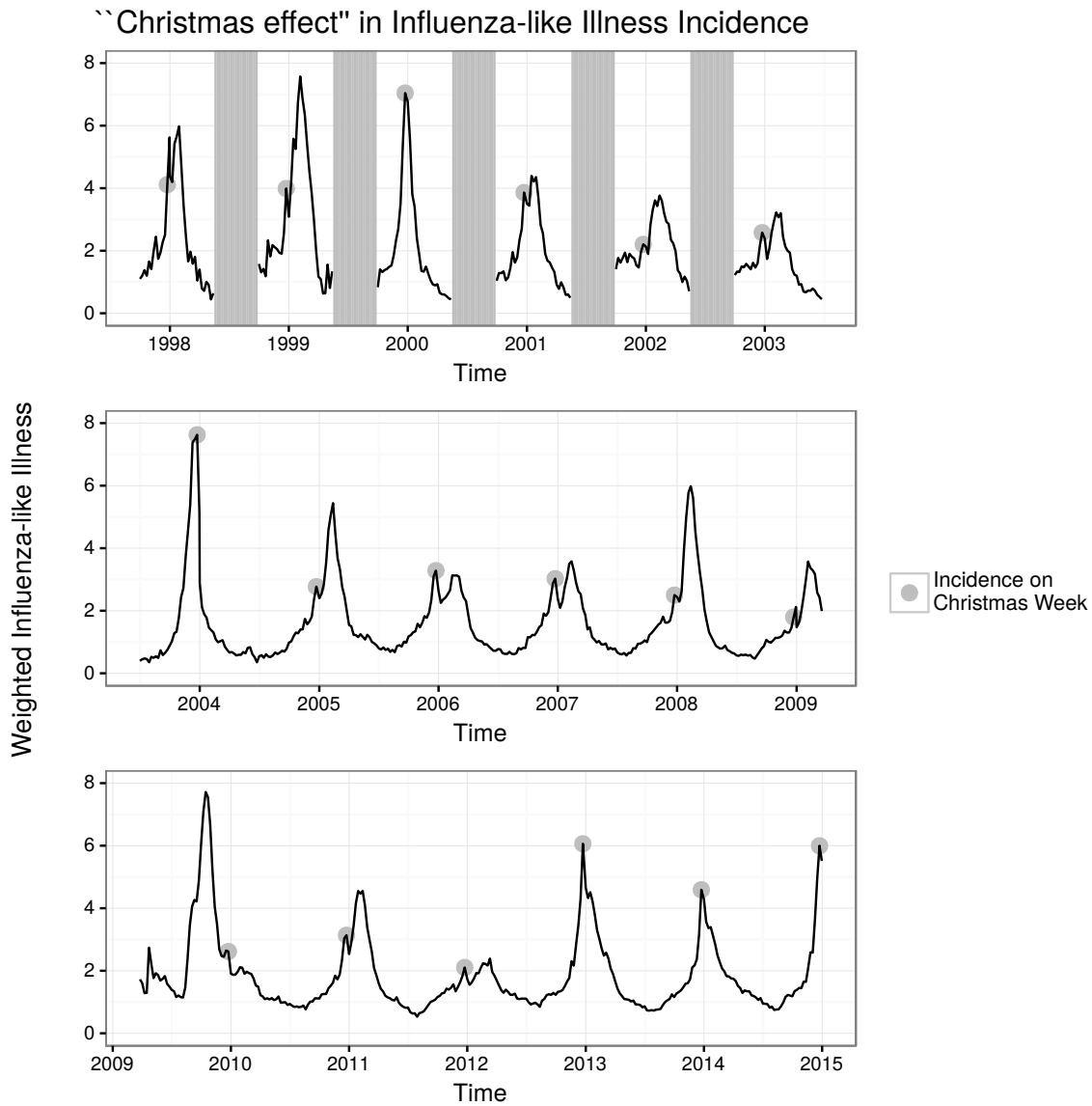
Figure 12: Illustration of short term peaks in influenza-like illness on Christmas week. In every season in the data set except for two, there is a local peak in incidence on the week of Christmas; this peak sometimes coincides with the season peak. In those two other seasons (1997/1998 and 2008/2009), there is still a peak in the incidence measure near Christmas, but the peak occurs in the week after Christmas.